13th International Conference on Greenhouse Gas Control Technologies, GHGT-13, 14-18 November 2016, Lausanne, Switzerland

Thermodynamic optimization and part-load analysis of the NET Power Cycle

Roberto Scaccabarozzi[a,b], Manuele Gatti[a], Emanuele Martelli[a]*

[a] Politecnico di Milano, Department of Energy, Via Lambruschini 4, 20156, Milano
[b] LEAP (Laboratorio Energia e Ambiente Piacenza), Via Nino Bixio 27/c, 29121, Piacenza

Abstract

This paper performs the thermodynamic optimization and part-load analysis of the NET Power cycle (also called Allam cycle), a natural-gas-fired oxy-combustion cycle featuring 100% CO_2 capture level, very high net electric efficiency, and potentially near-zero emissions level. To determine the maximum achievable cycle efficiency and optimal cycle variables, an Aspen Plus flowsheet including accurate first-principle models of the main equipment units has been developed and combined with a black-box optimization algorithm. The corresponding maximum cycle efficiency is equal to 55.35% (with 100% CO_2 capture). Optimization-based sensitivity analyses are performed to explore the neighborhood of the maximum efficiency cycle design with the aim of finding combinations of the cycle variables which lead to reduced costs and thermo-mechanical stress of the most critical components. Finally, the part-load performance of the optimized NET Power cycle has been analyzed. Results indicate that in the load range 100-40% the cycle (excluding the ASU) features a considerably lower efficiency decrease compared to a standard combined cycle. This result, showing the possibility of efficiently operating the cycle also at part-loads, further increases the attractiveness of the NET Power cycle.

Keywords: oxy-turbine; CO_2 capture; supercritical CO_2 cycle; part-load analysis; cycle optimization

* Corresponding author. Tel.: +39 0523356813.
E-mail address: emanuele.martelli@polimi.it

1. Introduction

Among the available carbon capture technologies, turbine-based oxy-combustion cycles appear to be a promising midterm solution for the production of electricity from natural gas. The oxy-combustion technology is based on a thermodynamic cycle in which the fuel is burned in a combustor with an oxidant stream composed mainly of pure oxygen. In a conventional plant the combustion is performed using air as oxidant, but the significant amount of nitrogen contained dilutes considerably the CO_2 in flue gases. It is well known that this is one of the major drawbacks affecting the energy consumption related to CO_2 Capture and Storage [1,2]. On the other hand, thanks to the removal of nitrogen from the oxidant, oxy-combustion cycles deal with working fluids featuring higher CO_2 concentrations, which may reduce the energy intensity of CO_2 separation. Nowadays, among the most interesting solutions proposed in literature for oxy-combustion cycles there are the ones based on CO_2-rich and H_2O-rich streams as working fluids. In the former case CO_2 capture is performed simply by splitting part of the main flow, while in the second case water condensation produces a stream rich in carbon dioxide, which then can be easily captured via partial condensation (however in both cases a further purification step may be required depending on CO_2 purity specifications).

Allam et al. [3] developed a highly regenerative supercritical cycle called "NET Power cycle" or "Allam cycle". The turbine inlet temperature is controlled by recycling a large amount of supercritical CO_2 to the combustor while heat recovery of the turbine exhaust gases is performed using a multi-flow heat exchanger (the regenerator). In [4] the developers estimated a cycle efficiency for natural gas combustion of 59% for the single combustor scheme (without reheat) and about 57.5% for the double combustor scheme (with reheat).

According to [5], the NET Power cycle is the most promising option both in terms of efficiency and economics. The main advantages of this cycle are the limited total specific plant cost (1560 €/kW) and the very high net electric efficiency which yield to a cost of electricity of 83.6 €/MWh, the lowest among the oxy-turbine cycles analysed in [5]. The attractiveness of the cycle is also due to its simplicity and limited number of components compared to other fossil-fuel systems with CO_2 capture.

The objectives of this study are:

   i) determine the optimal cycle variables and the corresponding maximum electric efficiency achievable by the NET Power cycle;

   ii) explore promising combinations of the cycle variables which allow to reduce the costs (and/or research and development efforts) of the equipment units while maintaining close-to-optimal efficiency;

   iii) assess the performance of the cycle when running at part-load.

Having a high part-load efficiency is very important to successfully operate the plant in today's electricity market.

2. NET Power cycle

The NET Power cycle scheme, as first presented by Allam et al. in 2011 [6], is represented in Fig. 1.
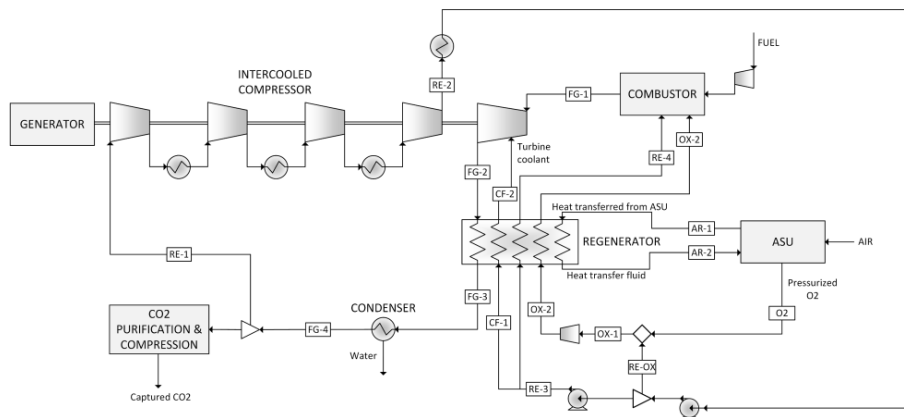

Fig. 1: Scheme of the analysed NET Power cycle.

Almost pure oxygen (99.5% purity, molar basis) pressurized at 120 bar is supplied by a cryogenic Air Separation Unit (ASU) (stream O2) and then it is mixed with a stream of recycled CO_2 (stream RE-OX), preheated to approximately 720°C in the regenerator and sent to the combustor. Oxygen is mixed with CO_2 before being preheated in the regenerator for safety reasons. The combustor operates between 200 bar and 400 bar and the firing temperature is moderated by injecting a large recycle stream of CO_2 (stream RE-4). Hot combustion gases at temperatures above 1100°C enter a cooled turbine featuring a limited expansion pressure ratio, between 6 and 12. Flue gases at approximately 700-800°C and 30-60 bar enter a multi-flow heat exchanger (the regenerator) which allows to efficiently recover the available heat by preheating the recycle streams (streams RE-3, OX-2) as well as the turbine cooling flows (stream CF-1). At the exit of the regenerator, the exhaust stream is cooled close to ambient temperature in a cooler which condenses and separates the water. The remaining stream (stream FG-4) is essentially pure CO_2 in the gas phase. Part of this stream is separated and sent to CO_2 purification, compression and storage, while the majority (stream RE-1, around 95% of stream FG-4) is compressed and recycled back to the combustor as temperature moderator. The intercooled compressor pressurizes the recycle stream to about 80 bar and the aftercooler takes it to near ambient temperature. Since these conditions are supercritical (dense phase CO_2) and correspond to a very high density of about 700 kg/m^3, the compression from 80 bar to the combustor pressure is performed with multi-stage centrifugal pumps. A stream of CO_2 at 120 bar (stream RE-OX) is extracted and mixed with the pressurized O_2 provided by the ASU. It must be noted that there is a lack of heat in the regenerator: the heat released by the exhaust low pressure stream is lower than the one required by the high pressure recycle stream. The cause of this difference (which is the opposite situation compared to conventional regenerative gas turbines) is that the specific constant pressure heat capacity of CO_2 increases with pressure, especially at low temperatures [4]. Part of the heat required is supplied by the condensation of water in the turbine exhaust gas. This phenomenon occurs within the regenerator at temperatures below 150°C. The remaining fraction of the heat deficit is covered by the air cooler of the cryogenic ASU: the main air compressor can make available hot air at 270°C, if it is not intercooled. According to the cycle developers [3], even though such an arrangement increases the power consumption of the ASU main air compressor, the overall effect on the cycle efficiency is positive. Heat is transferred from the ASU to the regenerator by a loop of heat transfer fluid, such as thermal oil.

3. Methodology for cycle optimization

The objective of the analysis is to find the cycle variables (pressures, temperatures, mass flow rates) which lead to the maximum net electric efficiency of the overall system (including ASU). The optimization problem can be stated as follows.

Objective function: maximum net electric efficiency of the cycle.

Independent optimization variables:
- turbine inlet pressure;
- turbine outlet pressure;
- flow rate of the recycle stream (stream RE-4 in Fig. 1; this variable influences the turbine inlet temperature);
- regenerator outlet temperature of the recycle and oxidant streams;
- regenerator outlet temperature of the expander cooling flow.

Nonlinear constraints:
- the minimum temperature difference at the hot end of the regenerator must be ≥ 20°C;
- the minimum temperature difference in the low temperature section of the regenerator must be ≥ 5°C;
- maximum allowed turbine outlet temperature = 860°C;
- heat balance and heat integration feasibility of the regenerator (computed with the methodology described in Section 3.2).

Bound constraints:
- turbine inlet pressure: between 200 bar and 400 bar;
- turbine outlet pressure: between 20 bar and 60 bar;
- combustor recycle flow rate: between 200 kg/s and 1000 kg/s;
- regenerator outlet temperature of the recycle and oxidant streams: between 500°C and 840°C;
- regenerator outlet temperature of the expander cooling flow: between 60°C and 500°C.

The cycle optimization problem is tackled with the black-box approach [7]: a derivative-free optimization algorithm explores the solution space of independent decision variables and, for each sampled solution, the process simulation software calculates the cycle and returns as output its performance. In other words, the process simulation software works as a black-box function called each time by the optimization algorithm to calculate the performance of the cycle.

The model of the NET Power cycle was developed in Aspen Plus V8.8 [8], a commercial sequential modular process simulation software licensed by AspenTech. On the basis of the analysis reported in [9], the Peng-Robinson equation of state was selected to calculate the fluid properties. Among the cycle components (compressors, pumps, expander, heat exchangers, etc.), the turbine and the regenerator required the definition of ad hoc models while the other equipment units were modelled with the blocks readily available in Aspen Plus. The same basis of design and performance assumptions adopted in [9] are used in this analysis.

3.1. Turbine model

To estimate the performance of the NET Power cycle (power output, turbine outlet temperature and mass flow rates of the cooling flows) the expander model must be able to properly handle the real gas effect (i.e., with an equation of state), and it should have only a few calibration parameters, without requiring detailed geometrical information of the stages, since such details are not yet available.

In [9], the same authors adapted the continuous expansion model proposed by El-Masri [10] for standard gas turbines. In particular, the following modifications were made:

    i) the model is implemented in Aspen Plus and it can handle any type of equation of state;
    ii) the number of expansion steps is finite so as to allow a numeric integration of the solution (the overall set of equations needs to be solved by means of a numerical algorithm);
    iii) the model accounts for the total pressure loss caused each time cooling flows are injected in the mainstream.

The model was calibrated to reproduce the performance of a frame "F" gas turbine using as reference the results obtained with the stage-by-stage model developed by Chiesa and Macchi [12,13]. Full details about the turbine model and its calibration can be found in [9].

3.2. Regenerator

Considering the fact that the multi-flow heat exchanger handles several streams with variable heat capacity and different inlet and outlet temperatures, and that water starts condensing within the component, multiple pinch-points (which actually limit the heat recovery process and then the temperature at which the cold streams are preheated) may exist in the regenerator. Thus the regenerator cannot be simply modelled as a multi-flow heat exchanger and, in order to maximize the heat recovery, a heat integration method is necessary. For this reason, the systematic heat integration methodology of Papoulias and Grossmann [13] has been adopted in this work: each hot/cold stream is divided into 20 temperature zones, and the maximum heat recovery problem (across all the temperature zones of all streams) is rigorously formulated as a linear program. Given the inlet and outlet temperatures and mass flow rates of the hot and cold streams of the regenerator as well as the minimum heat recovery approach temperature, the heat integration methodology determines the minimum required heat duty of the cold utility (cooling water) and hot utility (e.g., boiler). Since in the NET Power cycle there is not a boiler to provide additional heat to the regenerator (such a boiler would generate CO_2 emissions), cycle designs requiring a hot utility are classified as infeasible by the black-box optimization algorithm (PGS-COM) and rejected. This occurs for cycle designs featuring too high outlet temperatures of the recycle streams (to reach the outlet temperature of the cold streams set by PGS-COM, the heat available in the flue gases is not sufficient and a boiler would be necessary). Across the iterations, PGS-COM adjusts the outlet temperatures of the recycle streams so as to preserve feasibility of the heat integration in the regenerator while maximizing the cycle efficiency. For the low temperature section of the regenerator (T ≤ 300°C) a minimum temperature difference of 5°C has been considered, while 20°C for the high temperature section (T ≥ 600°C). A linear correlation has been used within the range 300-600°C.

Compared to the study recently proposed in [9] which has a less fine discretization of the regenerator (just three sections), the heat integration methodology adopted here allows to achieve an improved heat integration (hence a

slightly higher cycle efficiency, as shown in Section 4).

3.3. Optimization approach and PGS-COM algorithm

Compared to the equation oriented approach [7], the black-box strategy for process/plant optimization may considerably increase the probability of determining the global optimum because the optimization level considers only the independent decision variables (a few ones) and design specification constraints, since all the dependent variables (e.g., stream properties) and equipment equations (e.g., energy and mass balance equations) are hidden into the process simulation model (i.e., the black-box). On the other hand, the process simulation may fail to reach convergence or crash for some combinations of the input variables. Moreover, the output of the process simulation model may be non-smooth (non-differentiable or discontinuous) and noisy. Besides, due to the possible failures of the process simulation, some function evaluations may fail causing convergence issues of the optimization algorithm. Among the available black-box optimization algorithm, PGS-COM [14], a very robust hybrid derivative-free evolutionary algorithm, was selected because of its superiority on constrained non-smooth black-box problems. The algorithm combines the positive features of the constrained particle swarm optimizer [15], generating set search [16], and Complex [17]. PGS-COM has been successfully applied to tackle the optimization of a number of power cycles (e.g., organic Rankine cycles) and CO_2 capture processes (e.g., Rectisol, Selexol, etc.).

4. Optimized cycle

Table 1 compares the main performance and the most significant parameters of the optimized cycle with respect to those of the maximum efficiency cycle found by the same authors in [9] and the case simulated in [5]. Thanks to the improved heat integration of the regenerator, this newly optimized cycle improves by 0.55 percentage points the efficiency of the solution initially found in [9] without appreciable differences in the optimal values of the cycle variables. On the other hand, even though the efficiency figures are similar, the cycle variables adopted in [5] are significantly different from the optimal ones found in this work and in [9]. This suggests that the efficiency of the cycle is remains fairly constant in the region around the maximum efficiency solution.

Table 1: Performance results and most significant cycle variables of the Net Power cycle optimized in this work compared to the optimal version of [9] and [5].

	Unit	Results of this work	Results of [9]	Results of [5]
Thermal energy of feedstock (LHV)	MW$_{th}$	768.31	768.31	768.31
Turbine power output	MW$_e$	609.4	609.7	631.95
Recycle flow compressors consumption	MW$_e$	94.57	99.19	103.95
NG compressor	MW$_e$	4.03	3.97	4.75
Air separation unit	MW$_e$	85.56	85.52	85.45
Net electric power output	MW$_e$	425.26	421.06	422.95
Net electric efficiency (LHV)	%	55.35	54.80	55.05
Turbine inlet pressure	bar	288.69	283.62	300
Turbine outlet pressure	bar	47.02	47.15	34
Combustor outlet temperature	°C	1127.7	1123.8	1150
Turbine outlet temperature	°C	782.7	783.8	740
Final temperature of cooling flows	°C	163.95	162.95	284
Turbine inlet mass flow rate	kg/s	1491.8	1513.7	1264.7
Turbine cooling flows, total mass flow rate	kg/s	98.3	96.9	145
Total recycle mass flow rate (with oxygen)	kg/s	1573.6	1532.7	1393.1

To further explore this region, the optimization was repeated for a number of scenarios assuming progressively more conservative upper limits for the Turbine Outlet Temperature (TOT) and the maximum pressure of the cycle. The TOT limit, representative of the maximum allowed metal temperature in the last section of the turbine and in the regenerator hot end (therefore related to the usage of expensive materials), is reduced from 800°C to 650°C. The maximum pressure, which should affect the mechanical resistance and cost of the regenerator, combustor and first section and casings of the turbine, is reduced from 400 bar to 200 bar. For each new more conservative case the optimization of the cycle variables was repeated.

The result of this optimization-based sensitivity analysis are represented in Fig. 2. It shows that, for TOT limits above 725°C, it is not advantageous to increase significantly the pressure above 250 bar, since the net electric efficiency gains only a minor improvement above that limit. On the other hand, the difference of efficiency between cases with different turbine inlet pressure becomes considerable when the TOT limit is reduced below 725°C. Among the cases shown in Fig. 2, the case with turbine inlet pressure limited to 250 bar and TOT limited to 725°C appears quite promising as it preserves close-to-maximum efficiency while significantly reducing the thermo-mechanical issues of the regenerator.

It is important to note that, as shown by the same authors in [9], the efficiency of the NET Power cycle strongly depends on the specific power consumption of the ASU, minimum temperature difference of the regenerator, and on the effectiveness of the turbine cooling system. The efficiency figures reported in this paper refer to the same assumptions made in [9].
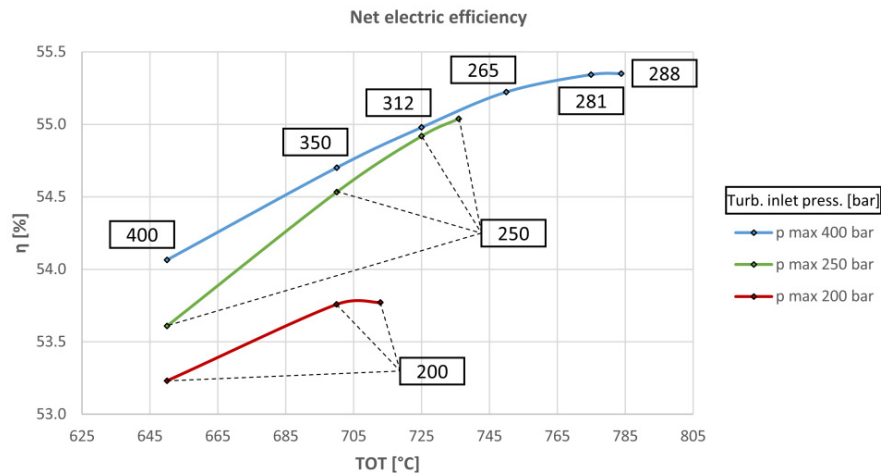

Fig. 2: Net electric efficiency of optimized cycles featuring different sets of allowed maximum turbine inlet pressure and TOT. The labels report the optimal turbine inlet pressures.

5. Part-load analysis

5.1. Off-design models and control strategy

In order to reproduce the NET Power performances in part-load conditions, starting from the optimized case, the models of the units of the Aspen Plus flowsheet have been modified in order to reproduce the off-design behavior of the cycle components (heat exchangers, turbine, compressors, pumps). It is important to note that in this analysis the part-load behavior and performance of the ASU have not been modelled and investigated. The strong assumption at the basis of this analysis is that the ASU can operate at 40% load maintaining the same specific energy consumption as the full load operation.

As for the regenerator, first it was necessary to assess the heat transfer area $A_{i,j}$ between each hot stream i and cold stream j. The regenerator has been divided in 9 temperature zones and for each zone k the thermal power $Q_{i,j,k}$

exchanged between hot stream *i* and cold stream *j* has been determined. For each stream, the value of the convective heat transfer coefficient has been assumed on the basis of literature data ([18,19]) and the resulting global heat transfer coefficient $U_{i,j}$ has been determined neglecting the metal resistance. Knowing $Q_{i,j,k}$ and $U_{i,j}$ and the inlet/outlet temperatures of the streams, first $A_{i,j,k}$ and then the total area across the different zones ($A_{i,j}$ = sum of the $A_{i,j,k}$) have been determined for the full-load condition. At part-load, the heat transfer area remains constant while the global heat transfer coefficient $U_{i,j}$ changes depending on the mass flow rates of the two streams and the pressures (see Eq.(1) [18,20]):

$$U_{i,j} = \cfrac{1}{\cfrac{1}{h_i^{fl}}\left(\cfrac{p_i^{fl}}{p_i}\right)^{0.5}\left(\cfrac{m_i^{fl}}{m_i}\right)^{0.8} + \cfrac{1}{h_j^{fl}}\left(\cfrac{p_j^{fl}}{p_j}\right)^{0.5}\left(\cfrac{m_j^{fl}}{m_j}\right)^{0.8}} \tag{1}$$

On the basis of the above-determined $U_{i,j}$ and $A_{i,j}$, the regenerator model determines the outlet temperatures of the hot and cold streams. Also intercoolers and the condensers have been modelled in a similar way, considering the variation of the *U* coefficient due to the variation of mass flow rate of the cycle working fluid.

The off-design curve of the expander can be simplified assuming that the non-dimensional mass flow rate, defined in Eq.(2), remains constant [21]:

$$\varphi = \frac{m\sqrt{zRT}}{D^2 p} = cost. \tag{2}$$

where *m* is the inlet mass flow rate, *z* is the compressibility factor, *T* is the Turbine Inlet Temperature (TIT), *D* is the turbine diameter, *p* is the turbine inlet pressure. Being a simplified analysis aimed at a preliminary assessment of the cycle performance at part-load, off-design variations of expansion efficiency of the turbine stages have been neglected.

As far as the two main compressors are concerned, the recycle compressor and the CO_2 compressor, we assumed that both compressors feature Variable Inlet Guide Vanes (VIGV) to reduce the fluid mass flow rate without stalling. Compression efficiency variations due to the rotation of the VIGVs have been neglected.

Given the operational constraints of the units, for fixed fuel input, the cycle has two independent control variables:
  i) minimum cycle pressure (turbine outlet pressure);
  ii) VIGV angle.

In other words, the mass flow rate of the recycle stream (main stream of the cycle) can be reduced at part-loads either reducing the minimum pressure of the cycle or closing the VIGV of the recycle compressor. Since decreasing the minimum cycle pressure leads to operational issues of the CO_2 compressor (which needs to operate at a higher pressure ratio so as to reach the specified final CO_2 delivery pressure), in this analysis we focus on a control strategy which keeps constant the minimum cycle pressure: keeping constant the minimum pressure of the cycle, the VIGV of the recycle compressor are adjusted so as control the mass flow rate of the recycle stream.

For fixed fuel input, the position of the VIGV (i.e., recycle stream mass flow rate) can be optimized to maximize the part-load efficiency of the cycle. On the other hand, as the VIGV are closed, the pressure ratio of the cycle decreases (the turbine inlet pressure depends on the inlet mass flow rate of fluid, as shown in Eq.(2)) causing a considerable rise of the turbine outlet temperature (as it happens for standard gas turbines with the VIGV control mode) with resulting mechanical issues of the last turbine stages and regenerator. Thus, when optimizing the VIGV position, it is necessary to check and limit the increase of TOT.

5.2. Part-load results

Due to the above-mentioned increase of TOT at part-loads, four different scenarios have been considered with maximum allowed TOT equal respectively to the full-load value (783°C), 800°C, 825°C, and 850°C. The net electric efficiency, normalized with respect to the full-load value, is reported in Fig. 3 while the independent and dependent control variables are plotted in Fig. 4. Fig. 3 highlights that, at low power outputs, i.e., when fuel input is below 80%, the limit on the TOT can affect significantly the performance of the cycle, which can be up to 1.6% points higher if the TOT allowed can be increased up to 850°C (the efficiency at 40% thermal rating increases from 46.1% to 47.7%).
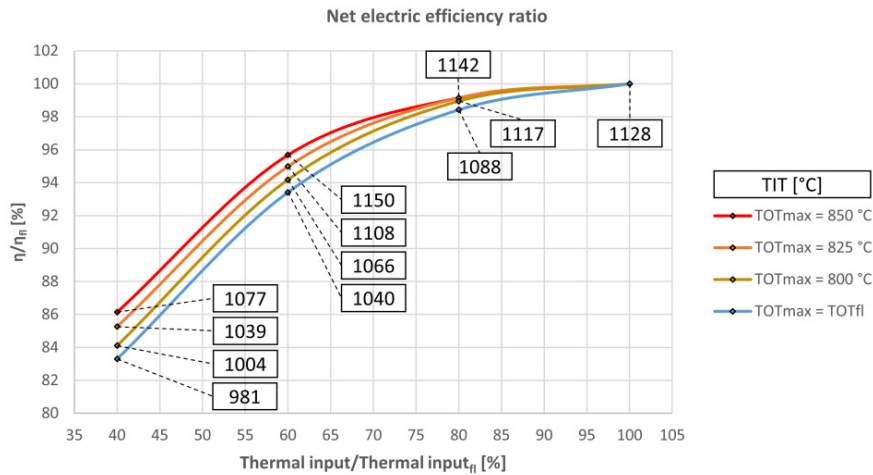
Fig. 3: Normalized net electric efficiency as a function of the normalized fuel input for the devised control strategy considering four different values of maximum allowed turbine outlet temperatures (TOT). The y-axis represents the ratio between the net electric efficiency at part-load and the full-load value. The x-axis is the ratio between the fuel input at part-load and the full-load value. The part-load performance of the ASU has been neglected.

As indicated by the figures of TIT reported in Fig. 3, in the case with TOTmax = 850°C (red line) the position of the VIGV is optimized so as to keep the TIT close or even higher than to the full-load condition. In this control strategy with high allowed TOT, the decrease of efficiency at part-load is mainly due to the increase of heat transfer irreversibility occurring in the regenerator and increase of thermal power rejected to the environment.

The left-hand side plot of Fig. 4 shows the trend of the variables adjusted as a function of the power rating according to the control strategy described in Section 5.1. It shows that the outlet pressure has been fixed for all part-load operation, whereas the other controlled variable, the mass flow rate of the recycle stream decreases almost linearly. The right-hand side plot of Fig. 4 represents the profile of the most significant dependent variables resulting from the application of the control strategy. In the case with the minimum limit on TOT (blue lines), the TIT and the expander inlet pressure fall almost linearly with the fuel input. On the other hand, in the case with high TOT allowed (red lines), the TIT is even slightly increased between 60% and 80% load until the maximum TOT constraint is activated.
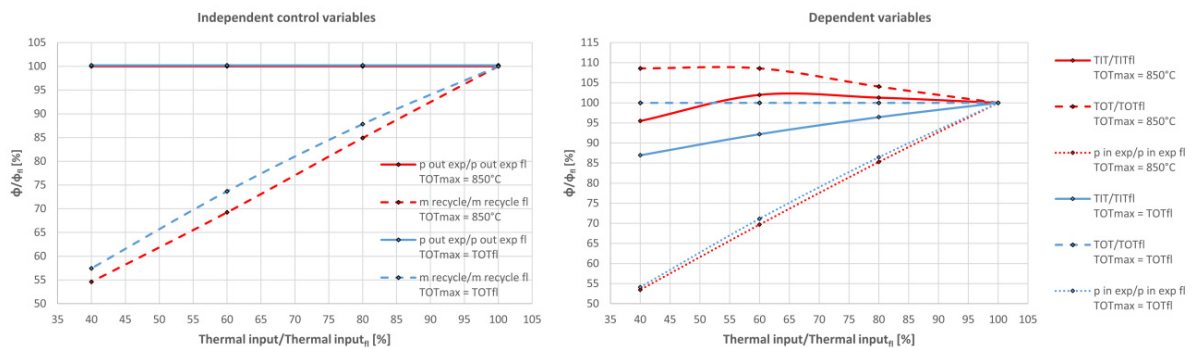

Fig. 4: Normalized values of the most significant operating variables at various part-load fuel inputs (the subscript fl indicates full load variables). The independent variables are degrees of freedom which are optimized for each part-load operation, whereas the dependent variables are a result of the control strategy adopted.

Fig. 5 compares the normalized part-load efficiency of the NET Power cycle against the one of a state-of-the art

combined cycle without CO_2 capture based on a GE 9FB followed by a triple pressure level heat recovery steam cycle with reheat. The part-load simulation of the combined cycle has been performed using Thermoflex [22]. The GT control load strategy set by Thermoflex combines both the VIGV closure and the TIT reduction to limit the raise of TOT. Results are in line with those reported in [23].

The comparison highlights that, even though the full-load net electric efficiency of the combined cycle (58.35 %) is slightly higher than the one of NET Power considered in this study, the efficiency drop at part-load of the conventional combined cycle is larger, especially in the range 60-80% load. The difference in efficiency is even larger if the control strategy with TOT limited to 850°C is considered for the NET Power cycle. The main advantage of the NET Power cycle is the lower impact of the TIT decrease on the cycle efficiency.
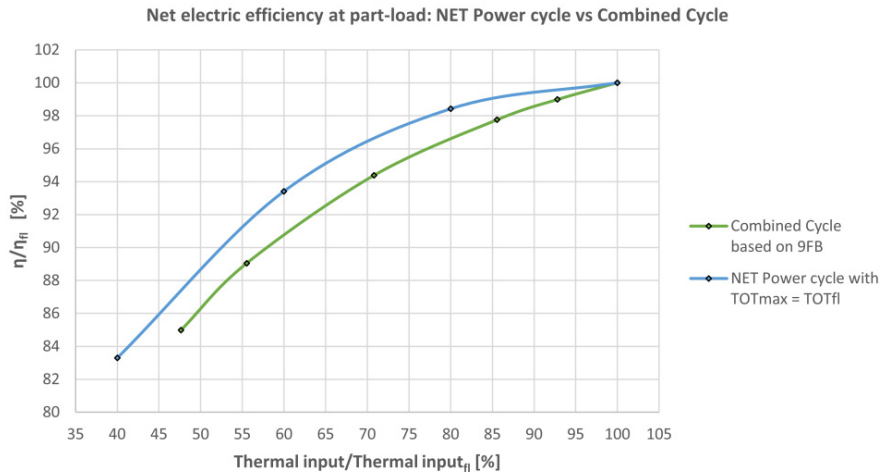

Fig. 5: Comparison between the normalized net electric efficiency of the Net Power cycle and a triple-pressure level combined cycle when operating at part-load. The y-axis represents the ratio between the net electric efficiency at part-load and the full-load value. The x-axis is the ratio between the fuel input at part-load and the full-load value. The part-load performance of the ASU has been neglected.

6. Conclusions

The study presented in this work has shown that the NET Power cycle is a very interesting option to implement CO_2 capture from natural gas. Indeed, in addition to avoid CO_2 as well as other emissions, the cycle features really high efficiency figures not only at full-load but also at part-loads.

The systematic cycle optimization study has shown that the cycle variables can be adjusted so as to maintain close-to-maximum cycle efficiency with reduced thermo-mechanical stress of the equipment units. For example, the optimized solution with a turbine inlet pressure limited to 250 bar and the TOT limited to 725°C achieves a net electric efficiency only 0.43 percentage points lower than the maximum efficiency cycle.

Results of the part-load analysis indicate that in the load range 100-40% the cycle (excluding the ASU) benefits from a considerably lower efficiency decrease compared to a standard combined cycle indicating the possibility of achieving a high operational flexibility. This result further increases the attractiveness of the NET Power cycle. Further research studies need to take into account the detailed part-load performance variation of the ASU.

References

[1]   A. Kyle, J. Black, M. Woods, N. Kuehn, W. Shelton, and W.-C. Yang, "Carbon Capture Approaches for Natural Gas Combined Kyle, Allison; Cycle Systems," 2010.

[2]   M. Finkenrath, "Cost and Performance of Carbon Dioxide Capture from Power Generation," 2011.

[3]   R. J. Allam, M. R. Palmer, G. W. Brown, J. E. Fetvedt, D. A. Freed, H. Nomoto, M. Itoh, N. Okita, and C. Jones, "High Efficiency and

Low Cost of Electricity Generation from Fossil Fuels While Eliminating Atmospheric Emissions, Including Carbon Dioxide," *Energy Procedia*, vol. 37, pp. 1135–1149, 2013.

[4]   R. J. Allam, J. E. Fetvedt, B. A. Forrest, and D. A. Freed, "The Oxy-Fuel, Supercritical CO2 Allam Cycle: New Cycle Developments to Produce Even Lower-Cost Electricity From Fossil Fuels Without Atmospheric Emissions," in *ASME Turbo Expo 2014: Turbine Technical Conference and Exposition*, 2014, p. V03BT36A016.

[5]   N. Ferrari, L. Mancuso, J. Davison, P. Chiesa, E. Martelli, and M. C. Romano, "Oxy-turbine for Power Plant with CO2 capture," in *13th International Conference on Greenhouse Gas Control Technologies, GHGT-13*, 2016.

[6]   R. J. Allam, M. R. Palmer, and G. W. Brown, "System and method for high efficiency power generation using a carbon dioxide circulating working fluid," Patent US 2011/0179799 A1, 2011.

[7]   L. T. Biegler, I. E. Grossmann, and A. W. Westerberg, *Systematic Methods of Chemical Process Design*, 1st ed. Upper Saddle River, New Jersey 07458, 1997.

[8]   "AspenTech website." [Online]. Available: http://www.aspentech.com/products/aspen-plus/. [Accessed: 07-Oct-2016].

[9]   R. Scaccabarozzi, M. Gatti, and E. Martelli, "Thermodynamic analysis and numerical optimization of the NET Power oxy-combustion cycle," *Appl. Energy*, vol. 178, no. 0, pp. 505–526, Sep. 2016.

[10]   M. A. El-Masri, "On Thermodynamics of Gas-Turbine Cycles: Part 2—A Model for Expansion in Cooled Turbines," *J. Eng. Gas Turbines Power*, vol. 108, no. 1, pp. 151–159, 1986.

[11]   "GECOS - Group Energy COnversion Systems website." [Online]. Available: http://www.gecos.polimi.it/software/gs.php. [Accessed: 07-Oct-2016].

[12]   P. Chiesa and E. Macchi, "A Thermodynamic Analysis of Different Options to Break 60% Electric Efficiency in Combined Cycle Power Plants," *J. Eng. Gas Turbines Power*, vol. 126, no. 4, pp. 770–785, 2004.

[13]   S. A. Papoulias and I. E. Grossmann, "A structural optimization approach in process synthesis—II," *Comput. Chem. Eng.*, vol. 7, no. 6, pp. 707–721, Jan. 1983.

[14]   E. Martelli and E. Amaldi, "PGS-COM: A hybrid method for constrained non-smooth black-box optimization problems," *Comput. Chem. Eng.*, vol. 63, pp. 108–139, Apr. 2014.

[15]   Xiaohui Hu and R. Eberhart, "Solving Constrained Nonlinear Optimization Problems with Particle Swarm Optimization," in *6th World Multiconference on Systemics, Cybernetics and Informatics 2002*, 2002.

[16]   R. M. Lewis, A. Shepherd, and V. Torczon, "Implementing Generating Set Search Methods for Linearly Constrained Minimization," *SIAM J. Sci. Comput.*, vol. 29, no. 6, pp. 2507–2530, Jan. 2007.

[17]   J. Andersson, "Multiobjective Optimization in Engineering Design: Applications to Fluid Power Systems," Linköpings universite, 2001.

[18]   D. G. Ulrich and P. T. Vasudevan, *Chemical Engineering Process Design and Economics: A Practical Guide*, 2nd ed. Process Publishing, 2004.

[19]   Y. Liang, D. Che, and Y. Kang, "Effect of vapor condensation on forced convection heat transfer of moistened gas," *Heat Mass Transf.*, vol. 43, no. 7, pp. 677–686, Mar. 2007.

[20]   F. Capra and E. Martelli, "Numerical optimization of combined heat and power Organic Rankine Cycles - Part B: Simultaneous design & part-load optimization," *Energy*, vol. 90, pp. 329–343, 2015.

[21]   S. L. Dixon and C. Hall, *Fluid Mechanics and Thermodynamics of Turbomachinery*, 7th ed. Elsevier Inc., 2014.

[22]   "Thermoflow website." [Online]. Available: https://www.thermoflow.com/combinedcycle_TFX.html. [Accessed: 07-Oct-2016].

[23]   T. S. Kim, "Comparative analysis on the part load performance of combined cycle plants considering design performance and power control strategy," *Energy*, vol. 29, no. 1, pp. 71–85, Jan. 2004.